

NUCLEOSYNTHESIS IN LOW- AND INTERMEDIATE-MASS STARS: AN OVERVIEW

Nami Mowlavi

Geneva Observatory, CH-1290 Sauverny, Switzerland

Abstract. An overview of the main phases of the evolution of low- and intermediate-mass stars is presented, and the different types of nucleosynthesis operating from the pre-main sequence up to and including the asymptotic giant branch phase described. The surface abundance modifications brought by each nucleosynthesis process is also briefly discussed.

To appear in: *Tours Symposium on Nuclear Physics III*, Ed. H. Utsunomiya, Amer. Inst. of Phys., 1997 (*invited review*)

I INTRODUCTION

Low- and intermediate mass (LIM) stars are defined as those who end their life without proceeding through the carbon and heavier elements burning phases. Part of them experience only the core H-burning phase, ending their life as He white dwarfs (WDs). This is the case for stars with initial masses between ~ 0.08 and $\sim 0.5 M_{\odot}$ (M_{\odot} being the solar mass). Stars with masses between ~ 0.5 and $6 - 8 M_{\odot}$, on the other hand, proceed further to the core He-burning phase, and end as C-O WDs. Stars less massive than $\sim 0.08 M_{\odot}$ never reach central temperatures high enough to ignite H, and end as brown dwarfs. Stars more massive than $\sim 10 M_{\odot}$ (called massive stars), on the other hand, continue their evolution through central C and heavier element burning, eventually ending their life in a supernova explosion. The mass limits defining these categories are obtained through evolutionary model calculations (e.g. [19]). They are still subject to some uncertainties mostly due to the shortcomings in the mixing prescriptions and mass loss rates. As for stars with initial masses between $6 - 8$, their fate is still uncertain. We refer to [19] for a discussion (see also [16,15]).

In this paper, we consider the evolution of *single* stars with masses between ~ 0.5 and $6 - 8 M_{\odot}$ (the case of massive stars is reviewed by G. Meynet in this volume). The nucleosynthesis operating in these LIM stars involve mainly the light elements up to Al, and the *s*-process elements. Because of the high mass loss rates characterizing the late stages of the evolution of these stars, the nuclides synthesized in their deep interior, and dredged-up to the surface, efficiently contribute to the

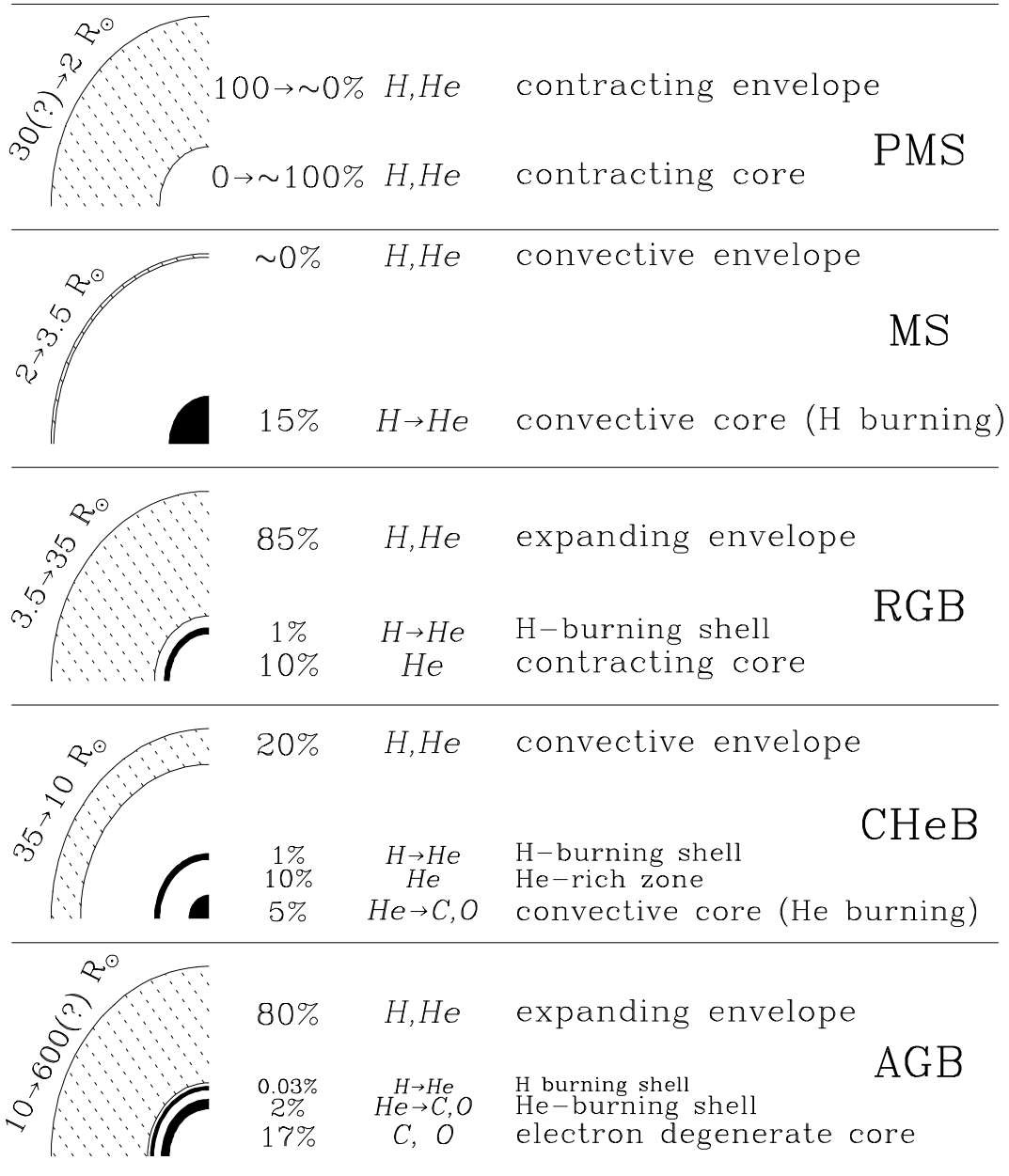


FIGURE 1. Schematic representations of the structure of a star at different phases of its evolution. The numbers on the upper left of each diagram indicate the variation of the surface radius during the considered phase of evolution. The columns on the right of each diagram indicate, from left to right, the percent of the total mass of the star contained in the given region, its main chemical composition and a description of it. hatched areas in the diagrams indicate convective regions, while filled areas denote regions where nuclear energy is produced. The quantities refer to a $3 M_{\odot}$ $Z=0.02$ star. Adapted from [21].

chemical enrichment of the interstellar medium. Such is the case for He, ${}^7\text{Li}$, C, N, ${}^{19}\text{F}$, ${}^{26}\text{Al}$, and the *s*-process elements.

This paper aims at presenting a general overview of the nucleosynthesis occurring in LIM stars. A more detailed review of the subject is presented in [22]. The main phases of the structural evolution of these stars are presented in Sect. II, while Sect. III analyses the nucleosynthesis operating in the different phases of their evolution. Some concluding remarks on surface abundance predictions in LIM stars are discussed in Sect. IV.

II STRUCTURAL EVOLUTION

The structure of a $3 M_{\odot}$ $Z=0.02$ model star, with Z being the mass fraction of all elements heavier than He (called the “metallicity”), is displayed in Fig. 1 at different phases of its evolution. Five phases are distinguished:

1) The *pre-main sequence (PMS) phase*, which constitutes the overall contraction phase prior to H ignition in the center. It is characterized by an accretion phase during which mass from a circumstellar disk is accreted on the forming star ([5] and references therein), and an increasing central temperature until H ignites in the core at $12 \lesssim T_6 \lesssim 25$ (where T_6 is the temperature expressed in units of 10^6 K). The chemical composition is homogeneous throughout the star, except for some of the light nuclides (up to C) which already burn at temperatures of a few 10^6 K.

2) The *main sequence (MS) phase*, characterized by the transformation of H to He in the core. It represents the star’s longest duration phase. The core is convective for stars with $M \gtrsim 1.2 M_{\odot}$, while H burns radiatively in lower mass stars.

3) The *red giant branch (RGB) phase*, which follows the MS phase. As a result of core contraction, the radius of the star increases and its surface temperature decreases. Hydrogen burns now in a shell surrounding a H-depleted core. *Low-mass stars* ($M \lesssim 2 M_{\odot}$), defined as those containing an electron-degenerate core at this phase of their evolution, may pass as much as 20% of their life as red giants. For *intermediate-mass stars* ($M \gtrsim 2 M_{\odot}$), on the other hand, this phase is short, generally less than 7% of the MS lifetime. This phase is also characterized by the convective envelope penetrating into the deep layers, the material of which has been affected by H-burning. The ashes of H-burning are thus mixed to the surface. This is called the “*first dredge-up*”.

4) The *core He-burning (CHeB) phase*, characterized by the transformation of He to C and O in a convective core surrounded by a thin H-burning shell. This is the second longest lived phase in the life of the star. In low-mass stars, He ignition proceeds in a degenerate core, which leads to a thermal runaway called “*core helium flash*”.

5) The *asymptotic giant branch (AGB) phase*, following the CHeB phase. He-

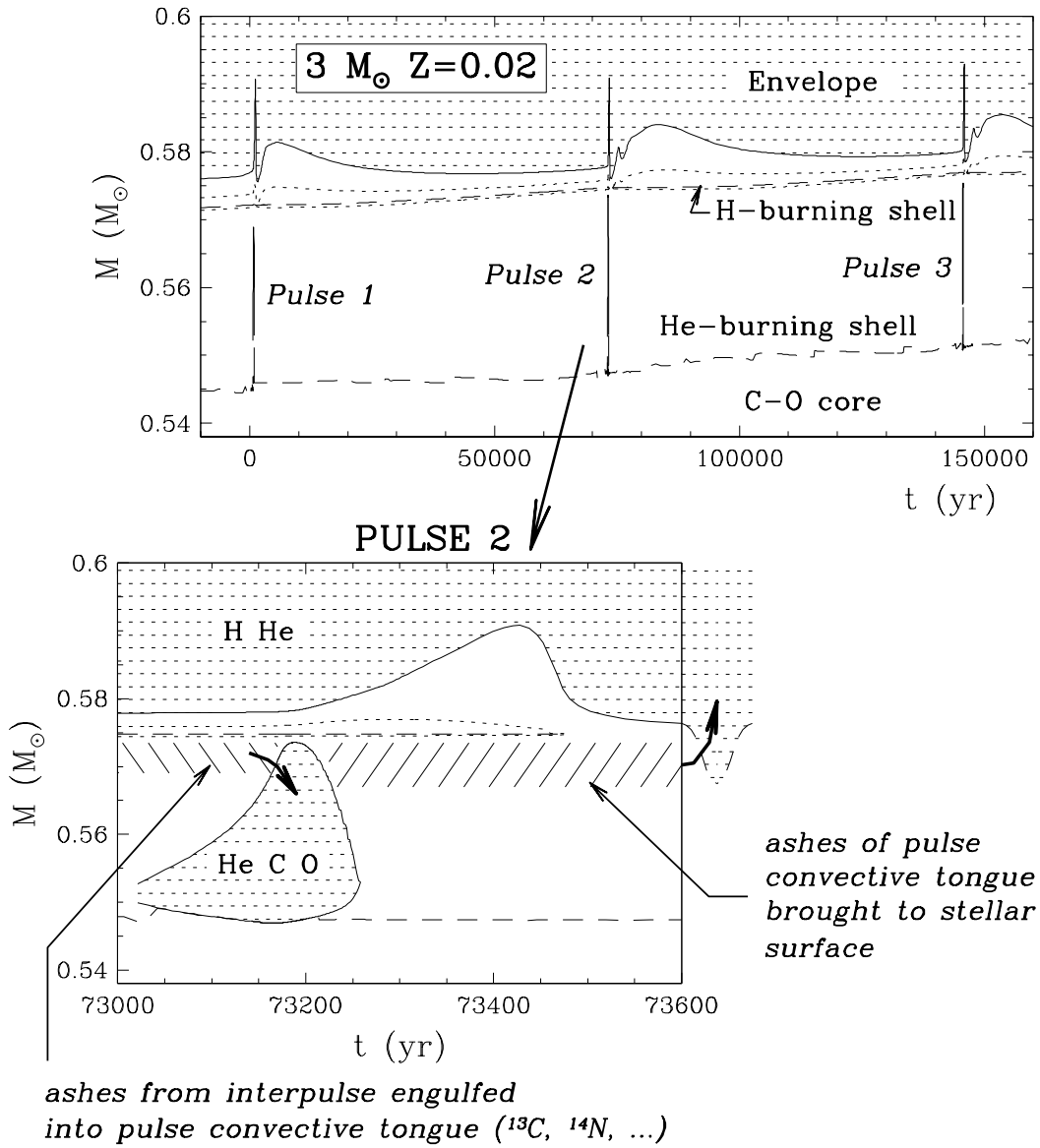


FIGURE 2. *Upper panel:* Structural evolution of a $3 M_{\odot}$ $Z=0.02$ AGB star, during the first three thermal pulses in the He-burning shell. Filled areas denote convective regions. The long-dashed lines locate the maximum energy production in the H-burning (top) and He-burning (bottom) layers. Short-dashed lines locate the extensions of the H-burning shell, defined by the region where the energy production exceeds $1 \text{ erg g}^{-1} \text{ sec}^{-1}$. The three vertical lines in the He-burning shell denote the occurrence of the thermal instabilities. *Lower panel:* Enlargement of the structural evolution during the second pulse of the $3 M_{\odot}$ $Z=0.02$ star. A third dredge-up is simulate on the outer right-hand side of the panel. The hatched region to the left of the pulse indicates the layers containing the ashes left behind by the H-burning shell during the interpulse phase, and which are injected into the pulse. The layers containing the ashes of the pulse and which are mixed into the envelope are delimited by the hatched region on the right of the pulse. Adapted from [21].

lithium now burns in a shell and the star becomes a red giant for the second time. The envelope penetrates in the deep layers and, in stars more massive than about $4 M_{\odot}$, the products of H burning are transported for the second time to the surface (“*second dredge-up*”). The star is now characterized by an electron degenerate C-O core of mass between 0.5 and $1.2 M_{\odot}$, one thin He-burning shell capped by a thin H-burning shell, and a deep convective envelope. The nucleosynthesis and energy production are confined to a region comprising less than 3% of the total mass of the star. A distinctive feature of the AGB phase is the fact that the He-burning shell becomes thermally unstable (see Fig. 2) and liberates, periodically and on a short time-scale (several tens of years), 10^2 to 10^6 times the energy provided by the H-burning shell. These energy bursts are called “pulses”. They lead to the development of a convective zone in the He-burning shell. The quiescent evolutionary phase, or “interpulse” period, lasts several 10^4 years.

The lower panel of Fig. 2 gives an enlargement of the convective regions during a thermal instability. The thermal pulses have two important consequences. From a chemical point of view, the material synthesized in the He-burning shell is convectively mixed with layers close to the H-burning shell. The layers left behind by the H-burning shell (hatched region on the left of the pulse in Fig. 2), containing the ashes of that combustion phase, are engulfed by the pulse and contribute to a rich nucleosynthesis therein.

From a structural point of view, an important envelope response is predicted to occur after the pulse extinction. The convective envelope penetrates into the H-burning shell, and can even reach the H-depleted regions. Eventually, it can sink into the carbon-rich layers. The material processed by the pulse could then be transported to the surface. This scenario is called the “*third dredge-up*”.

III NUCLEOSYNTHESIS

A During the PMS phase

Nuclear reactions involving light elements from D to C begin to occur in PMS stars at temperatures varying from $T_6 = 1$ to 12. The case of deuterium is of particular interest in relation with Big Bang Nucleosynthesis. This element burns at $T_6 \sim 1 - 1.5$, mainly through $D(p, \gamma) {}^3\text{He}$. As a result, the total mass of D + ${}^3\text{He}$ is conserved. This property, together with the fact that D is not produced in Galactic environments, has been, and still often is, used to derive an information on primordial D abundance (e.g. [32] and references therein).

Let us also mention the case of ${}^6\text{Li}$ and ${}^7\text{Li}$, which burn in the deep layers by p-capture at $T_6 \sim 3$. To what degree the surface Li is affected depends on the initial stellar mass and on various physical conditions such as mixing or rotation. We refer to [20,11] and references therein for a discussion on this issue.

B From the MS up to the AGB phase

As far as stellar surface abundances and interstellar chemical enrichment are concerned, H burning is the only nucleosynthesis process of interest in LIM stars from the MS up to the AGB phase. Indeed, the nuclides produced by He burning during the CHeB phase remain trapped into the white dwarfs.

Four non-explosive H-burning modes have been identified to date (e.g. [28]): the pp-chains, the “cold” CNO cycles, and the NeNa and MgAl chains. The pp-chains and CNO cycles are the main contributors to the energy production. The pp-chains are dominant at $T_6 \lesssim 20$ (i.e. in the cores of MS stars with $M \lesssim 1.2 M_\odot$), and the CNO cycles at higher temperatures (i.e. in the cores of MS stars with $M \gtrsim 1.2 M_\odot$, and in the H-burning shells). When the latter cycles are active in the central regions of MS stars, convection develops in the core due to the steep temperature dependence of the energetics of the CNO reactions. All the four modes, however, are of importance from a nucleosynthetic point of view.

The pp-chains are described at length in the literature (see [10,2] for a general description, and [4,12] for a discussion related to the “solar neutrino problem”). We discuss here only the implications of this mode of H burning in relation with ${}^3\text{He}$. In addition to its production through D burning during the PMS phase (see Sect. III A), ${}^3\text{He}$ is produced in low-mass stars¹ by $p(p, e^+ \nu) D(p, \gamma) {}^3\text{He}$. This occurs essentially in stellar regions where $T_6 \lesssim 15$ (in deeper layers where the temperatures are higher, ${}^3\text{He}$ is destroyed by ${}^3\text{He}({}^3\text{He}, 2p) {}^4\text{He}$ or ${}^3\text{He}(\alpha, \gamma) {}^7\text{Be}$), and which are engulfed by the first dredge-up. Low-mass stars would thus be important contributors to the galactic ${}^3\text{He}$ enrichment. According to current galactic chemical evolution models, however, this leads to a present interstellar ${}^3\text{He}$ abundance prediction much higher than what is observed (e.g. [33,24,26]). We refer to [22] for a more extensive discussion on this subject.

Hydrogen burning by the CNO cycles operates mainly through the transformation of ${}^{12}\text{C}$ and ${}^{16}\text{O}$ to ${}^{14}\text{N}$ ([10], see also G. Meynet in this volume). We refer to [3] for a description of the cycles and their yields, as well as for a discussion of the uncertainties still affecting the involved reactions rates. Two nuclides, ${}^{13}\text{C}$ and ${}^{17}\text{O}$, play an important role in confronting stellar model predictions with observations. The nuclear transformation of ${}^{12}\text{C}$ to ${}^{14}\text{N}$ proceeds first through the production of ${}^{13}\text{C}$ by ${}^{12}\text{C}(p, \gamma) {}^{13}\text{N}(\beta^+) {}^{13}\text{C}$, and then through its destruction by ${}^{13}\text{C}(p, \gamma) {}^{14}\text{N}$ (see Fig. 1 of [3]). As a result, ${}^{13}\text{C}$ is overproduced in intermediate layers of LIM stars, and destroyed in deeper regions ([22]). The same is true for ${}^{17}\text{O}$, which is produced by ${}^{16}\text{O}(p, \gamma) {}^{17}\text{F}(\beta^+) {}^{17}\text{O}$ and destroyed by ${}^{17}\text{O}(p, \alpha) {}^{14}\text{N}$. The surface abundances of both ${}^{13}\text{C}$ and ${}^{17}\text{O}$ are then increased by the first dredge-up scenario. Indeed, a severe decrease in the ${}^{12}\text{C}/{}^{13}\text{C}$ and ${}^{16}\text{O}/{}^{17}\text{O}$ ratios is observed at the surface of red giant stars (e.g. [13]).

¹) In stars more massive than $3 - 4 M_\odot$, the MS lifetime is shorter than the characteristic ${}^3\text{He}$ production time-scale, and no ${}^3\text{He}$ is produced. In these stars, ${}^3\text{He}$ is essentially destroyed in the deep layers

Arnould, Mowlavi and Champagne [3] have also reviewed the NeNa and MgAl chains. These become mainly active at $T_6 \gtrsim 40$. The first of these chains contributes to the production of ^{23}Na by proton capture on ^{22}Ne . The second one is of importance, prior to the AGB phase, in the production of ^{27}Al from ^{25}Mg and, at $T_6 \gtrsim 65$, from ^{24}Mg . Overabundances of both ^{23}Na and ^{27}Al are also confirmed at the surface of red giants (e.g. [31,8,25]).

C During the AGB phase

The nucleosynthesis occurring in AGB stars is summarized in Fig. 3. Four sites can be distinguished:

1) The first site is obviously the H-burning shell during the interpulse period. The ashes of that combustion are brought to the surface through the third dredge-up scenario. The temperature in the H-burning shell increases with time, and reaches values above T_6 . In those conditions, the MgAl chain leads, in particular, to an efficient production of ^{26}Al ([14]). The interest in this nuclide resides both in relation to γ -ray line astronomy (e.g. [27]) and to cosmochemistry (e.g. [1,18]).

2) The He-burning shell constitutes the second obvious nucleosynthesis site. It contributes mainly to the production of ^{12}C through the 3- α process. The carbon is brought by the convective tongue of the thermal pulses to regions close to the H-burning shell. Successive occurrences of the third dredge-up scenario are then responsible for a gradual surface carbon enrichment, turning eventually a M star (whose surface C/O ratio is less than 1) into a C star (with C/O>1).

Another important contribution from the He-burning shell is provided by the nucleosynthesis resulting from the injection into the pulse of the H-burning shell ashes. In particular, the injection of ^{13}C leads to the production of neutrons through the $^{13}\text{C}(\alpha, n)^{16}\text{O}$ reaction. These neutrons can then be used to produce elements heavier than iron via the s-process nucleosynthesis, as well as ^{19}F (the nucleosynthesis path of which is described in [23]). Unfortunately, the amount of ^{13}C left behind by the H-burning shell turns out to be too low to result in any significant s-process nucleosynthesis, as well as to produce the fluorine in the amounts required by the observations ([23]).

3) An independent source of ^{13}C is expected to result from a partial mixing of protons into the carbon-rich region ([17]). This occurs below the convective envelope during a dredge-up scenario (see Fig. 3). When the temperature increases during the interpulse period, the protons are captured by ^{12}C and form ^{13}C . The low proton density prevents *all* of this ^{13}C to be transformed into ^{14}N . The surviving ^{13}C is most probably burned radiatively before the occurrence of the next pulse, leading to the production of ^{19}F and the s-process elements during the interpulse phase.

4) Finally, in stars more massive than about $4 M_{\odot}$, the temperature at the bottom of the envelope increases above $T_6 \sim 50$, activating the H-burning modes *within*

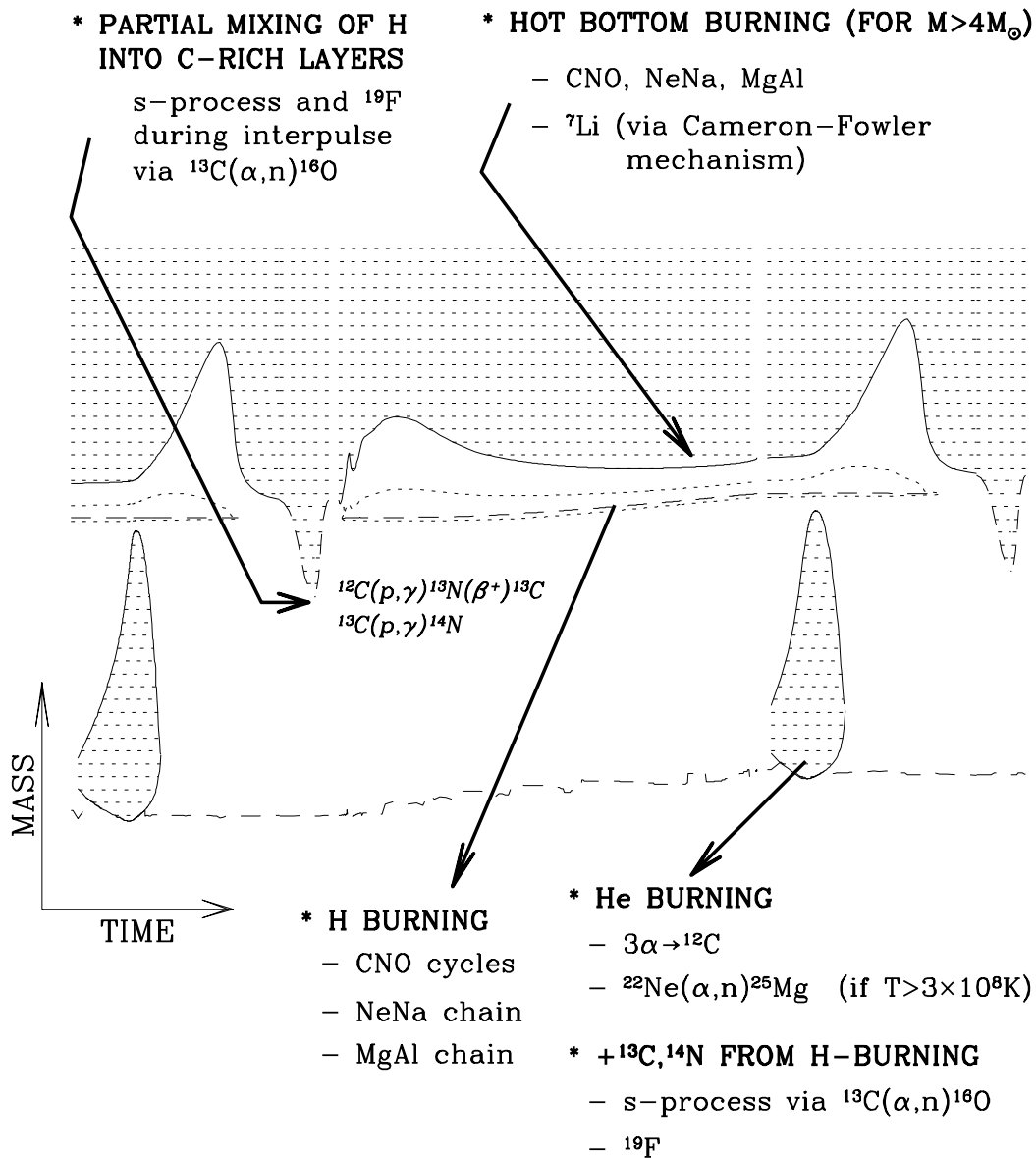


FIGURE 3. Overview of the nucleosynthesis occurring in AGB stars. The figure displays a schematic representation of two successive pulses. The interpulse phase is drawn on a much reduced time-scale, and lasts in reality *much* longer than each pulse. Hatched areas and dashed lines have the same meanings as in Fig. 2. Dredge-ups following each pulse (identified by the dashed envelope border) are also displayed. Adapted from [21].

the envelope. This phenomenon, known as hot bottom burning (HBB), modifies the surface composition without the need to invoke a dredge-up scenario. The signatures of HBB are quite characteristic. In particular, it can explain the low $^{12}\text{C}/^{13}\text{C}$ at the surface of some stars. It destroys ^{12}C and ^{18}O through the CNO cycles ([6]), and ^{19}F by $^{19}\text{F}(\text{p}, \alpha)^{16}\text{O}$ ([23]). It provides also an efficient site for the production of ^{26}Al through the MgAl chain. Moreover, HBB can lead to the synthesis of ^7Li through the Cameron and Fowler ([7]) mechanism, which combines the production of ^7Be at the bottom of the convective envelope by $^3\text{He}(\alpha, \gamma)^7\text{Be}$ and its convective transport to the surface where it is transformed to ^7Li by electron capture ([29]).

IV FINAL REMARKS

The first and second dredge-ups mix the ashes of hydrogen burning in the envelope. In contrast, the third dredge-up has the distinctive characteristic of bringing to the surface, in addition to the ashes from the H-burning shell, products resulting from helium burning. Nucleosynthesis occurring *in* the envelope, on the other hand, affects surface abundances without the need to invoke a dredge-up scenario. This concerns the light elements during the PMS phase, mainly D, ^3He and Li, or the elements involved in the CNO cycles and NeNa and MgAl chains in the case of HBB during the AGB phase.

Quantitative confrontation of surface abundance predictions from stellar models with various observations, however, reveal several disagreements which attest of our still poor knowledge of some physical processes occurring in the stars. The main shortcomings concern the mixing processes. Some examples in relation to LIM stars can be found in [34,9,30]. These are reviewed in more details in [22].

Finally, let us emphasize that the transition from the AGB to the post-AGB phase, during which the envelope of the AGB star is ejected and a planetary nebula eventually forms, is still poorly known. In particular, the history and rates of mass loss, whether the envelope is ejected intermittently or through a single “super wind” episode, and when this (these) strong wind(s) occur during the AGB phase, all limit the predictive capabilities of current AGB models concerning the final yields of LIM stars.

REFERENCES

1. Anders E., Zinner E., *Meteoritics* **28**, 490 (1993)
2. Arnould M., Mowlavi N.: 1993, in *Inside the Stars*, eds. Weiss W.W., Baglin A., ASP Conf. Ser. Vol. 40, pp 310-323 (1993)
3. Arnould M., Mowlavi N., Champagne A.: 1995, in *32nd Liège Int. Astroph. Coll.*,

- eds. Noels A., Fraipont-Caro D., Gabriel M., Grevesse N., Demarque P., pp 17-29 (1995)²
4. Bahcall J.N., in *“Neutrino Astrophysics”*, Cambridge University Press, Cambridge (1989)
 5. Bernasconi P.A., *A&AS* **120**, 57 (1996)
 6. Boothroyd A.I., Sackmann I.-J., Ahern S., *AJ* **418**, 457 (1993)
 7. Cameron A.G.W., Fowler W.A., *ApJ* **164**, 111 (1971)
 8. Cavallo R.M., Sweigart A.V., Bell R.A., *ApJ* **464**, L79 (1996)
 9. Charbonnel C. *ApJ* **453**, L41 (1995)
 10. Clayton D.D., in *“Principles of stellar evolution and nucleosynthesis”*, McGraw-Hill, New-York (1968)
 11. D’Antona F., Mazziteeli I., *ApJS* **90**, 467 (1994)
 12. Dzitko H., Turck-Chièze S., Delbourgo-Salvador P., Lagrange C., *ApJ* **447**, 428 (1995)
 13. El Eid M.F., *A&A* **285**, 915 (1994)
 14. Forestini M., Paulus G., Arnould M., *A&A* **252**, 597 (1991)
 15. Garcia-Berro E., Ritossa C., Iben I. *ApJ* **485**, 765 (1997)
 16. Hashimoto M., Iwamoto K., Nomoto K. *ApJ* **414**, L105 (1993)
 17. Herwig F., Bloeker T., Schoenberner D., El Eid M., *A&A* **324**, L81 (1997)
 18. MacPherson G.J., Davis A.M., Zinner E.K., *Meteoritics* **30**, 365 (1995)
 19. Maeder A., Meynet G., *A&A* **210**, 155 (1989)
 20. Martin E.L., Claret A., *A&A* **306**, 408 (1996)
 21. Mowlavi N., Ph.D. Thesis (unpublished)²
 22. Mowlavi N., in *Cosmic Chemical Evolution*, IAU Symp. 187, in press²
 23. Mowlavi N., Jorissen A., Arnould M., *A&A* **311**, 803 (1996)²
 24. Olive K.A., Schramm D.N., Scully S.T., Truran J.W., *ApJ* **479**, 752 (1997)
 25. Pilachowski C.A., Sneden C., Kraft R.P., Langer G.E., *AJ* **112**, 545 (1996)
 26. Prantzos N., *A&A* **310**, 106 (1996)
 27. Prantzos N., *A&A Sup.Ser.* **120**, 303 (1996)
 28. Rolfs C.E., Rodney W.S., in *Cauldrons in the Cosmos*, The University of Chicago Press, Chicago (1988)
 29. Sackmann I.-J., Boothroyd A.I., *ApJ* **392**, L71 (1992)
 30. Shetrone M.D., *AJ* **112**, 2639 (1996)
 31. Takeda Y., Takada-Hidai M., *PASJ* **46**, 395 (1994)
 32. Turner M.S., Truran J.W., Schramm D.N., Copi C.J., *ApJ* **466**, L59 (1996)
 33. Vangioni-Flam E., Olive K.A., Prantzos N., *ApJ* **427**, 618 (1994)
 34. Wasswerburg G.J., Boothroyd A.I., Sackmann I.-J., *ApJ* **442**, L21 (1995)

²⁾ postscript files available by anonymous ftp on ‘obsftp.unige.ch’ in the directory ‘pub/mowlavi’